Pergamon

Geochimica et Cosmochimica Acta, Vol. 68, No. 7, pp. 1489–1501, 2004

0016-7037/04 $30.00 + .00

doi:10.1016/j.gca.2003.10.011

Adsorption of thorium and protactinium onto different particle types: Experimental findings

WALTER GEIBERT* and REGINA USBECK

Alfred Wegener Institute for Polar and Marine Research, Am Handelshafen 12, 27570 Bremerhaven, Germany

(*Received July* 17, 2003; *accepted in revised form October* 6, 2003)

Abstract—Here we present the results of experiments investigating the adsorption of Protactinium and Thorium onto different particle types in natural seawater. Particle types studied were smectite as a representative of clay, biogenic opal from a cleaned diatom culture, manganese dioxide precipitate, and calcium carbonate. The particles were added to three different types of natural seawater (0.5 mg/L) which were first 0.2 μm-filtered, and the distribution of Pa and Th between dissolved and particulate phase (>0.2 μm) was monitored for 4 to 5 d at increasing time intervals. The tracers applied were the β-emitters ^{233}Pa and ^{234}Th. The measurement technique via β-counting for both nuclides in the same sample is reported here for the first time.

The observed recoveries during the experiment range from 40 to 99 ($\pm$5) % for Th and from 51 to 105 ($\pm$6) % for Pa. The distribution coefficients (K_d) after establishment of an equilibrium cover a wide range for Th from 0.5 to 107 $\times$ 10^6 ml/g, and from 0.03 to 166 $\times$ 10^6 ml/g for Protactinium, depending on particle type and on the type of seawater used.

Thorium revealed a specific affinity for all particle types investigated, with varying degree and adsorption kinetics. The results suggest that all particle types investigated may serve as Th carrier phases in the sediment. Pa was found to be less particle reactive than Th in most cases. Th/Pa fractionation factors ($F_{Th/Pa}$) were also obtained. Weakest fractionation was found on MnO_2 ($F_{Th/Pa}$=1), followed by the chemically cleaned biogenic opal (2.8) and smectite (5.4). The results for calcium carbonate were highly variable. Our experimental results imply that particle composition is indeed playing a role in the differing marine geochemistry of Th and Pa. We conclude that experiments with filtered natural seawater using particle concentrations on a natural level are a helpful approach when investigating the geochemical behaviour of strongly particle-reactive elements like Th and Pa in the marine environment.

1. INTRODUCTION

Thorium (Th) and protactinium (Pa) are radioactive elements that occur naturally in the ocean. Different Th- and Pa-nuclides with specific half-lives (^{234}Th: 24.1 d, ^{230}Th: 75200 yr, and ^{231}Pa: 32500 yr) are constantly supplied at a known rate to seawater by the decay of uranium. Uranium displays conservative behaviour under most oceanic conditions. In contrast, both thorium and protactinium are rapidly removed from seawater by particles, to which they -generally speaking- readily adsorb. Depending on the constant production rate of the respective Th- or Pa-nuclide, and on particle flux, a more or less pronounced radioactive disequilibrium between the progenitor (a uranium isotope) and its daughter nuclide develop. This disequilibrium, a depletion of Th or Pa in the water column with respect to uranium, or an enrichment of Th and Pa in the upper sediment layers, provides information about particle flux. This information is particularly precious because there are very few such tools available that enable us to convert concentrations (the property which is usually accessible to measurements) into fluxes (the parameter needed to calculate budgets).

Consequently, the longer-lived isotopes ^{230}Th and ^{231}Pa have been used to calculate a variety of variables in the context of particle flux, including sediment rain rates and sediment redistribution (Suman and Bacon, 1989; François et al., 1993; Thomson et al., 1993) or variations of productivity in space and time (Anderson et al., 1983a,b; Kumar et al., 1993, 1995). For a recent review on the applications of long-lived radionuclides of the U- and Th-series, see Henderson and Anderson (2003).

The shorter lived isotopes ^{234}Th and ^{228}Th (half-life 1.91 yr, a product of the ^{232}Th decay series) are used to calculate particle export from the surface layer (Tsunogai and Minagawa, 1976; Coale and Bruland, 1985; Buesseler et al., 1992; Rutgers van der Loeff et al., 1997); and particle recycling in the benthic nepheloid layer (Rutgers van der Loeff et al., 2002), and much has been learned about the interaction of different particle size classes (particulate-colloidal-dissolved) from the distribution of the short-lived thorium isotopes. Many works have shown that colloidal substances are involved in the adsorption and desorption of Th onto particles (Tsunogai et al., 1974; Li et al., 1984; Honeyman et al., 1988; Honeyman and Santschi, 1989; Baskaran et al., 1992; Tsunogai et al., 1994; Quigley et al., 2001). This fact is widely applied to investigate the role of colloids for oceanic biogeochemical cycles. A large fraction of Th is known to be adsorbed onto colloidal organic matter, as shown for example by Baskaran et al. (1992) or Guo et al. (1997). Several studies (Wen et al., 1997; Burd et al., 2000; Quigley et al., 2001) have pointed out the role of colloid aggregation and adsorption onto particles for the formation of larger aggregates. For a recent review of the applications of short-lived U- and Th-series nuclides, see Cochran and Masqué (2003).

However, it is not just particle flux and half-life which controls the distribution of thorium and protactinium. Other

* Author to whom correspondence should be addressed (wgeibert@awi-bremerhaven.de).

factors, still far from being quantitatively understood, have to be taken into account. These factors are, firstly, advection, mainly influencing the long-lived nuclides ^{230}Th and ^{231}Pa. Their residence time in the water column of the ocean is long enough to allow some lateral transport to occur before they are scavenged (Anderson et al., 1983a,b). Pa is much more affected by advection than Th, a fact that has been used to reconstruct circulation patterns of the past (Yu et al., 1996; Marchal et al., 2000). Secondly, and this is the issue to which this work is intended to contribute, the degree to which the composition of particles influences the distribution of ^{230}Th and ^{231}Pa in the oceanic environment is still a matter of debate.

The possible variability of the Th-distribution among different particle types has been a source of uncertainty in the interpretation of ^{230}Th-corrected particle fluxes in sediment traps as well as in the sediment itself. The same is true for estimations of carbon export from the euphotic zone of the ocean based on ^{234}Th, or the use of ^{231}Pa/^{230}Th as a paleoproductivity or paleocirculation proxy. Attempts to give a quantitative prediction of the distribution of a distinct radionuclide in a natural mixture of particles suffer from the extreme variability in particle properties. The whole complexity of natural particles must, for practical reasons, typically be reduced to a few characteristic parameters when describing their composition, e.g., %carbonate, %opal, %C_{org}, and %lithogenic (sometimes a synonym for "the rest"), or %sand, %silt and %clay. Obviously, these parameters have little to do with the physical or chemical properties actually useful for a quantitative description of trace metal adsorption such as the available surface area or the mineralogical composition of the clay fraction. The complex mechanistic description of trace element partitioning within a continuum of natural particles, if possible at all, conflicts with the coarse models we have to apply when using a proxy.

To obtain a practical solution for this problem, we have here divided the question of the influence of particle composition on Th and Pa scavenging here into three different questions, corresponding to three different applications. Concerning the use of ^{230}Th as a constant flux tracer, it is necessary to find out whether ^{230}Th is mainly scavenged by one or more distinct particle phases or whether it is distributed more or less homogeneously between different particles. If the latter is the case, it may be applied to normalize the flux of virtually any sedimentary component for redistribution, as has been done in the past (e.g., Frank et al., 1999; Chase et al., 2003b). Concerning the use of the ^{231}Pa/^{230}Th ratio as a proxy for paleoproductivity or paleocirculation, it should be clarified whether different particles will fractionate ^{230}Th and ^{231}Pa differently. For example, it has been proposed that opal is a phase preferentially scavenging ^{231}Pa compared to ^{230}Th (Walter et al., 1997; Chase et al., 2002; Lao et al., 1992), thus obscuring the paleoproductivity record in opal dominated regions (Walter et al., 1999; Chase et al., 2003a). The third, and most complex, question is derived from the application of short-lived Th isotopes as tracers for particle dynamics in the upper water layers. The question is whether the composition of the colloidal phase of seawater, presumably containing the largest fraction of Thorium in seawater, will influence the transfer of Th and Pa to the particulate phase and thus the behaviour of Th and Pa with respect to different particle types.

So far, almost all published attempts to answer the question of Th and Pa adsorption onto different particles have chosen to study the result of the adsorption process in natural particulate matter, either in the sediment or in sediment trap material. The few available experimental results on Th adsorption have not been designed to answer the above mentioned questions and are thus difficult to transfer to applications.

Here, we present experimental results on Th and Pa adsorption onto different particle types. The results shed light on some major problems linked to the use of thorium and protactinium in marine science. The experimental design presented here is shown to be a step towards more natural conditions in experimental approaches to the marine environment.

2. METHODS

2.1. Experimental Design

Previous attempts to investigate the adsorption of Pa and Th onto particles via experiments (Anderson and François, personal communication; and our own preliminary experiments) have revealed severe problems. Most problematic is the adsorption of the extremely particle-reactive Th onto the walls of the containers when using artificial seawater. Baskaran et al. (1992) had found evidence that adsorption onto container walls was considerably decreased when additional colloids were present in the sample. Experiments with filtered natural seawater still containing the original colloidal phase should therefore provide two advantages: First, only this type of experiment could give a realistic impression of the adsorption in natural systems and second, the adsorption of Th and Pa onto the container walls should be largely reduced if colloidal material is available in the sample.

A second difficulty in the design of such an experiment is the selection of an appropriate type of particles to give reproducible results, and to allow conclusions to be drawn about natural processes. In our experiments, four particle types were used. We chose a pure clay mineral (smectite) as representative for clay. For biogenic opal, a previously cleaned culture of a diatom (Thalassiosira) was selected as a representative. Besides clay and opal, calcium carbonate was included in the experiments as a further main component of marine sediments. Because manganese dioxide in the form of manganese crusts and manganese nodules plays a prominent role in paleoceanography and because this substance is widely applied in the sampling of natural radionuclides, this particle type was included as well. Additionally, one container was run without addition of particles to obtain a blank value. This sample is called "control run."

To find out whether the type of seawater used influences the adsorption behaviour of Th and Pa, the experiments were performed using three types of 0.2 μm filtered surface water during a cruise from Punta Arenas to Bremerhaven in May and June 2000 (RV *Polarstern* expedition ANT XVII/4). The water types were:

1. Surface water from the Argentine Basin sampled at 30°5.9′S, 26°5.7′W as a representative for a Subtropical Gyre
2. Surface water from a location close to the West African upwelling (20°13.2′N, 22°9.5′W, called WA) near the sites of the EUMELI-program (Morel, 1996) as a representative for a mesotrophic site.
3. Surface water from the North Atlantic (46°35′N, 14° 26.5′W, called NA), representing bloom conditions

To investigate the kinetics of the adsorption, subsamples were taken in increasing time intervals. For each subsample, Th and Pa were analyzed in the particulate and dissolved fraction. The complete sampling scheme is shown in Table 1.

2.2. Preparation of Particles

The smectite was a standard for determination of clay minerals via X-ray diffraction. To remove the large grains (mainly quartz) contained in the standard, a suspension of smectite in distilled water (>12 MΩ · cm) was prepared in a 30 cm high cylindrical glass and set aside for 1 d. The supernatant, containing the smallest size fraction, was decanted and retained, and the procedure was repeated. Afterwards, the milky

Table 1. Sampling and measurement scheme.

Step 1 →	Step 2 →	Step 3 →	Step 4 →	Step 5
natural seawater from 3 locations 0.2 μm filtered:	split in five 3-liter samples spikes added and these particles added, resp.:	each subsample split in two fractions:	From each sample 200 ml subsamples	3 measurements each fraction:
Argentine Basin (AB)	smectite	before particles were added	particulate (>0.2 μm)	^{234}Th
Off West Africa (WA)	biogenic opal	after 2 h	dissolved (<0.2 μm)	^{234}Th+^{233}Pa
North Atlantic (NA)	calcium carbonate	after 6 h		^{234}Th from ^{238}U
	MnO_2	after 14 h		
	control run	after 30 h		
		after 48 h		
		after 72 h		
		after 96 h		
		after 120 h (except AB)		

suspension obtained was filtered three times (0.2 μm Nucleopore cellulose acetate filters, 142 mm diameter) to separate the smectite from all particles <0.2 μm, which could otherwise be found in the dissolved phase during the experiments. After each filtration, the smectite was rinsed off the filter and resuspended. The concentration of the final suspension was determined by taking three small subsamples of known volume, which were dried and weighed.

The biogenic opal was obtained from several cultures of the diatom *Thalassiosira*. To destroy all organic material, the particles were first treated with H_2O_2 (30%), then with concentrated HNO_3. The particles were allowed to settle in a cylindrical vessel and the HNO_3 was decanted. The suspension obtained was repeatedly diluted with distilled water, set aside to allow the particles to sink out, decanted and filled up again until a pH of 5.5 was attained. Afterwards, particles <0.2 μm were separated and the particle concentration was determined as described for smectite. The obtained suspension formed a feltlike deposit at the bottom of the PE-bottle after storage, which could be brought back into suspension by vigorous shaking. Inspection of the particles under a microscope revealed mostly sickle-shaped fragments of the diatom frustrules. The original diameter of the diatoms was ~70 μm.

The carbonate particles were calcium carbonate *pro analysi* (p.a), obtained as a chemical reagent. The suspension was prepared in similar way to the opal suspension apart from the steps with H_2O_2 and acid, and filtered (0.2 μm) seawater from the North Sea was used instead of distilled water to rinse the particles.

The manganese dioxide particles were prepared by adding a solution of $MnCl_2$ to $KMnO_4$. The precipitate of MnO_2 was treated as described above to remove all particles <0.2 μm.

2.3. Thorium and Protactinium Spikes

The protactinium isotope used was ^{233}Pa, a β-emitter with a half-life of 27.0 d (Usman and MacMahon, 2000). The emitted electron has a maximum energy of 0.6 MeV. The ^{233}Pa spike was obtained by milking ^{233}Pa from a ^{237}Np-solution (following Anderson, personal communication). To ensure complete removal of HF in the spike, it was heated down several times to a small drop of fuming H_2SO_4, followed by a rinse with conc. HNO_3. The spike was stored in 4M HNO_3 and had a specific activity of 66.67 dpm/mL at 05/15/2000, 0:00 h.

The thorium isotope used was ^{234}Th, a β-emitter with a half-life of 24.1 d. The energy of the electron emitted by ^{234}Th is very weak, but its immediate daughter ^{234m}Pa (half-life 1.17 min) is also a β-emitter with a much higher energy of maximum 2.3 MeV (Nour et al., 2002). The decay of ^{234m}Pa was used for determination of ^{234}Th here. In fact, we added a uranium solution in 4 mol/L HNO_3 with a specific activity of ^{238}U of 783.2 dpm/mL in which ^{234}Th was in secular equilibrium. The samples had therefore to be corrected for the ingrowth of ^{234}Th from ^{238}U after sampling.

Immediately before addition of the spike mixture to the seawater samples, it was neutralized with NaOH 50% (s.p.) in a small PTFE beaker (5 mL volume) to avoid acidification of the seawater. This procedure was quantitative for the spikes (no loss on the walls of the PTFE beaker, as proven by recoveries). The only disturbing effect of the spiking procedure was the transient formation of small particles (not visible, but seen in particulate Th and Pa immediately after addition of the spikes). However, our results indicate that these particles (presumably $NaNO_3$) dissolved rapidly and had no influence on the further experimental results.

2.4. The Experiments

At the respective locations, ~20 L of seawater from the ship's seawater supply were collected in a polycarbonate container. The seawater supply had been run continuously. The container was previously cleaned mechanically and chemically (HCl 32%). The water was filtered (0.2 μm Nucleopore cellulose acetate filter, 142 mm diameter) and immediately filled via acid-cleaned tubes into another 20 L polycarbonate container similarly cleaned.

Five polycarbonate containers placed on magnetic stirrers were each filled with 3 L of the filtered seawater and the pH was determined with a glass electrode. All samples were stirred continuously with PTFE-coated magnets. Five portions of the spikes (Th and Pa mixed) were neutralized as described above and then immediately added to the samples. For the determination of particulate and dissolved Th and Pa (see Tab.1), a subsample of 200 mL was taken from the sample via a PE-spigot after the container had been shaken to bring particles adhered to the container walls into suspension. The first subsample was taken after the spikes had been added. Only then were the particles added to the samples to give a particle concentration of 0.5 mg/L, which is comparable to naturally occurring particle concentrations in the ocean. Higher particle concentrations would have led to very low dissolved fractions of the nuclides, resulting in large counting uncertainties. Subsamples were taken 2, 6, 14, 30, 48, 72, 96 and 120 h after the addition of the particles. Temperature was not actively controlled but can be assumed to be constant (air-conditioning in the ship's laboratory). The pH of the water was measured before each subsample was taken in the control run (no particles added) and occasionally checked in the particle suspensions for comparison (no differences found). The pH was found to decrease continuously from ~8.55 at the beginning of the experiment (after spiking) to 8.31–8.4 at the end of the experiment for all water types. The original pH of the filtered seawater was between 8.35 and 8.4 after filtration.

The subsamples were pumped over a 0.2 μm cellulose acetate filter (25 mm), followed by ~20 mL of distilled water (>15 M$\Omega \cdot$ cm) to include the part of the sample still in the in the pumping system, followed by an air bubble, which marked the end of the filtration and removed the water from the filter surface. Th and Pa measured on this filter is referred to as "particulate". The pump used for filtration was a KNF Flodos ND 300 diaphragm pump, max. flow rate 3 L $\cdot$ min^{-1}. The filtrate was filled into a 500 mL PE bottle. 50 μL of a 50 g/L $FeCl_3$-solution in 1 n HCl were added to the filtered subsample, followed by 3 drops of NH_4OH to form a precipitate of $Fe(OH)_3$ and

$Mg(OH)_2$. This coprecipitation technique is also used for quantitative recoveries when preparing samples for analysis of Th and Pa via α-spectrometry. The filtered subsample with the precipitate was set aside for at least 1 d to allow complete adsorption of all dissolved Th and Pa. Subsequently, the subsample was filtered under pressure over a 0.2 μm cellulose acetate filter as described above. The precipitate with Th and Pa remained quantitatively on the filter. Th and Pa measured in this precipitate is referred to as "dissolved".

All 25 mm filters were carefully taken out of the filtration system and placed upside down on a circular piece of thin polyethylene film (cling film) of 4 cm diameter. The border of the film was folded onto the "clean" side of the filter, leaving an area of 1.5 cm in diameter uncovered by the film. The filters were placed on a thin cover glass and placed on a hotplate (150°C) covered with Kleenex, covered with another layer of Kleenex and sealed in the PE film with gentle pressure until the filter was dry and the film started to stick to the paper. The samples obtained this way have an optimal shape for the following β-counting because of their size and their low and constant self-absorption due to their flat and constant shape. They can also be easily measured via γ-spectroscopy and are convenient for handling and storage.

2.5. Measurement of Th and Pa via β-Counting

The method to measure ^{234}Th and ^{233}Pa on the same sample via β-counting applied here has, to our knowledge, not been described previously. The method is based on the different energy of the electrons emitted by ^{233}Pa and the immediate daughter of ^{234}Th, ^{234m}Pa. Electrons emitted by ^{233}Pa have a considerably lower energy, leading to a rapid absorption by films of a certain thickness. We found that measurements of ^{233}Pa standards prepared similarly to our subsamples and covered by 6 layers of thick plastic film (as used for overhead transparencies) yielded only ~2% of the initial decays as compared to a standard covered with one layer of thin film. For ^{234}Th standards, still 43% of the initial events were detected with the thick cover. Therefore the samples were first counted under 6 layers of thick plastic film to calculate the amount of Th in the sample. Subsequently, the samples were measured under one layer of thin PE-film (cling film) to detect the decays of Th and Pa simultaneously. The fraction of Th decays can be determined from the initial measurement, and the remaining events were attributed to ^{233}Pa. The β-counter (GM-counter) used was a model from Risø Laboratories, Denmark, providing detectors for simultaneous measurement of five samples with 25 mm diameter (model GM25-5). This sea-going device has a background of 0.12 counts per minute (cpm).

One year after the cruise the samples were counted again to determine the uranium activity via ^{234}Th now grown into equilibrium. Then a small correction for ^{234}Th ingrown from ^{238}U between the sampling and the first measurement of ^{234}Th (max. 6 d) was performed. The decay of ^{234}Th between the measurement of ^{234}Th and ^{234}Th+^{233}Pa was also included in the calculations.

Despite the large number of measurements, calibration factors and corrections needed, the method has proven to be simple and reliable. The resulting error in Th and Pa concentrations from error propagation of counting statistics and uncertainty (1σ) in the calibration was found to be mostly below 5%. Larger errors occur in K_d values and in the fractionation factor especially if particulate and dissolved activities are very different, as the uncertainty increases at low activities.

We compared the results for Pa of 24 samples (particulate and dissolved) to measurements via γ-spectrometry. The analysis was done in our home lab on a Ge well type detector (effective volume 126 cm^3, full width at half maximum at 1.33 MeV: 2.05 keV). ^{233}Pa was measured at 312 keV (efficiency 33.7%). We found that the results agreed within the counting error for the samples and standards obtained by the above described $Fe(OH)_3$-precipitation. For the particulate samples, ^{233}Pa determined by β-counting turned out to be overestimated by 16% ($\pm$8%) when compared to γ-measurements. This effect can be attributed to the lower self-absorption compared to samples prepared with $Fe(OH)_3$. As the calibration of the β-counter was done with standards in $Fe(OH)_3$, activities of particulate samples not containing $Fe(OH)_3$ were initially overestimated. After the particulate samples had been corrected for this overestimation, an excellent agreement between the results of β-counting and γ-spectrometry was obtained (Fig. 1).

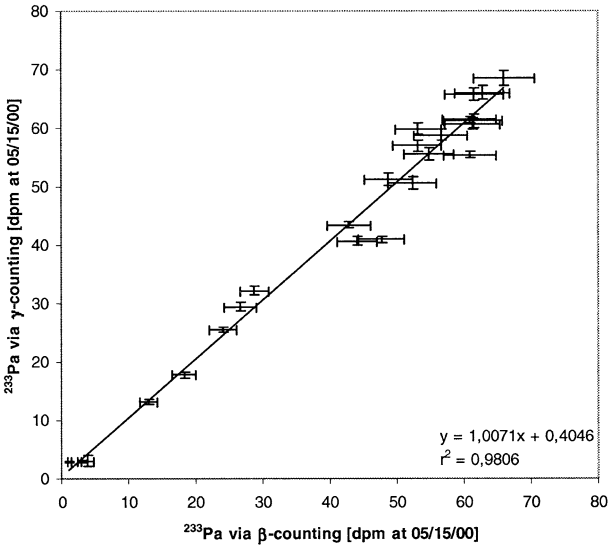

Fig. 1. Comparison of ^{233}Pa results from β-method described in text and corresponding γ-measurements

For ^{234}Th, no difference in efficiency between particulate samples and samples in $Fe(OH)_3$ was observed because of the higher energy of the electrons. A direct comparison of the two measurement techniques (as for ^{233}Pa) cannot be given for ^{234}Th because some ^{234}Th had ingrown from ^{238}U after the expedition and much of the initial ^{234}Th had decayed, leading to very large statistical errors in the γ-counting. However, the good agreement between ^{233}Pa via β-counting and γ-spectrometry implies that the initial ^{234}Th-values are also correct because the determination of ^{233}Pa via β-counting requires a precise value for ^{234}Th.

3. RESULTS

3.1. Recoveries

The recoveries of Th and Pa were calculated as the sum of measured activity in the particulate and dissolved fraction, compared to the initially added activity of the respective isotope. The observed recoveries for Thorium (Table 2, left side) range from 40 to 99%. Lowest recoveries were found in the samples with no particles added (control runs) and in the carbonate runs. There, obviously some loss to the container walls occurred. Smectite and opal particles yielded higher recoveries with values around 70%. Almost quantitative recoveries (with some exceptions towards the end of the experiments) are found in the MnO_2 run, indicating that MnO_2 shifts the Th-equilibrium between suspended particles and container walls virtually completely towards the suspended particles. Only for the last two MnO_2-subsamples in water from the North Atlantic a significant amount of MnO_2 particles (~30%) seems to get adsorbed onto the container walls. This loss is also seen for Pa. Generally speaking, little variation in recovery is seen between the different water types. Variation between the particle types is larger.

Protactinium recoveries (Table 2, right side) show a picture similar to Th. Recoveries for Pa are generally somewhat higher than for Th, indicating smaller losses to the container walls. Highest recoveries are again found for MnO_2.

Table 2. Recoveries of Th (left) and Pa (right) for all subsamples.[a]

		Thorium					Protactinium				
			Recovery (%)					Recovery (%)			
Site	Time (h)	Control run	Smectite	MnO_2	$CaCO_3$	Opal	Control run	Smectite	MnO_2	$CaCO_3$	Opal
Argentine Basin	0	51 ± 2	62 ± 3	60 ± 3	57 ± 3	66 ± 3	70 ± 3	71 ± 3	59 ± 3	68 ± 3	66 ± 3
	2	55 ± 3	44 ± 2	77 ± 4	49 ± 2	63 ± 3	64 ± 3	52 ± 2	77 ± 4	59 ± 3	61 ± 3
	6	67 ± 3	74 ± 3	96 ± 5	68 ± 3	70 ± 3	82 ± 4	83 ± 3	93 ± 5	80 ± 4	79 ± 3
	14	65 ± 3	59 ± 3	lost	60 ± 3	80 ± 3	77 ± 3	57 ± 2	lost	82 ± 4	83 ± 3
	23	65 ± 3	62 ± 3	88 ± 4	59 ± 3	66 ± 3	78 ± 4	82 ± 3	90 ± 5	67 ± 3	82 ± 4
	45	62 ± 3	77 ± 3	89 ± 4	60 ± 3	72 ± 3	76 ± 3	85 ± 3	97 ± 5	76 ± 3	73 ± 3
	68	54 ± 3	82 ± 4	95 ± 5	59 ± 3	71 ± 3	74 ± 3	84 ± 3	87 ± 5	77 ± 3	63 ± 3
	90	40 ± 2	74 ± 3	87 ± 4	56 ± 3	71 ± 3	63 ± 3	78 ± 3	95 ± 5	74 ± 3	74 ± 3
Off West Africa	−1	76 ± 3	79 ± 3	83 ± 3	81 ± 3	64 ± 3	91 ± 4	81 ± 4	81 ± 4	79 ± 4	67 ± 3
	2	75 ± 3	70 ± 3	87 ± 4	73 ± 3	77 ± 3	76 ± 3	78 ± 3	85 ± 4	79 ± 4	77 ± 3
	6	77 ± 3	79 ± 3	96 ± 5	78 ± 4	79 ± 3	75 ± 4	81 ± 4	98 ± 5	85 ± 4	79 ± 4
	14	77 ± 3	70 ± 3	97 ± 5	70 ± 3	76 ± 3	64 ± 3	68 ± 3	96 ± 5	71 ± 3	72 ± 3
	28	52 ± 2	75 ± 3	93 ± 4	54 ± 3	72 ± 3	51 ± 2	79 ± 3	95 ± 6	62 ± 3	61 ± 3
	46	65 ± 3	64 ± 3	90 ± 4	72 ± 3	83 ± 3	74 ± 3	97 ± 4	96 ± 6	76 ± 4	91 ± 4
	70	62 ± 3	71 ± 3	91 ± 5	60 ± 3	84 ± 4	69 ± 3	73 ± 3	87 ± 5	63 ± 3	84 ± 4
	94	73 ± 3	80 ± 4	95 ± 5	67 ± 3	79 ± 3	78 ± 4	81 ± 3	93 ± 6	82 ± 4	88 ± 4
	118	51 ± 2	72 ± 3	89 ± 4	58 ± 3	74 ± 3	57 ± 3	79 ± 3	84 ± 5	70 ± 3	82 ± 4
North Atlantic	−1	68 ± 3	80 ± 3	84 ± 3	74 ± 3	74 ± 3	69 ± 3	79 ± 4	79 ± 4	73 ± 3	72 ± 3
	2	61 ± 3	72 ± 3	96 ± 4	59 ± 3	58 ± 2	67 ± 4	68 ± 4	99 ± 5	73 ± 4	68 ± 3
	6	71 ± 4	81 ± 3	96 ± 4	76 ± 4	86 ± 4	67 ± 4	75 ± 4	93 ± 5	80 ± 4	83 ± 4
	15	83 ± 5	79 ± 3	96 ± 4	62 ± 4	80 ± 4	81 ± 5	79 ± 4	105 ± 6	80 ± 4	75 ± 4
	29	60 ± 3	76 ± 3	99 ± 5	62 ± 3	68 ± 3	74 ± 4	66 ± 3	95 ± 6	73 ± 4	67 ± 3
	47	65 ± 3	80 ± 3	94 ± 4	68 ± 3	84 ± 3	65 ± 4	67 ± 3	104 ± 6	89 ± 5	87 ± 4
	71	59 ± 3	74 ± 3	87 ± 4	68 ± 3	74 ± 3	78 ± 4	70 ± 3	89 ± 5	68 ± 4	82 ± 4
	95	58 ± 3	74 ± 3	71 ± 4	62 ± 3	59 ± 3	61 ± 3	85 ± 4	75 ± 5	80 ± 4	83 ± 4
	119	53 ± 2	69 ± 3	60 ± 3	57 ± 3	63 ± 3	66 ± 3	84 ± 4	70 ± 4	65 ± 3	60 ± 3

[a] Each of the three horizontal panels represents a different water type. The respective time after addition of the particles is given at the left side of the table.

3.2. Thorium on Different Particles

The percentages given for the particulate fraction of thorium were calculated as the particulate activity of thorium (Th_{part}) divided by the sum of dissolved and particulate thorium. The obtained values cover virtually the full range of possible results, from 4 to 98% (Fig. 2).

Some very low particulate activities imply that adsorption of Th onto the filter when separating particulate and dissolved phase was not taking place.

The most striking feature is the similar temporal pattern of adsorption for distinct particle types, although in some cases on different levels depending on the type of seawater used.

Another interesting finding with consequences for further interpretation of the results is the outcome of the control runs with no particles added (Fig. 2a). Here, a considerable fraction of Th was found in the particulate phase, sometimes more than in samples with particles added.

This control run was intended to serve as a blank value to be subtracted from the results. The obtained "blanks" as shown here can obviously not be used that way, not only because they are sometimes higher than for the other runs, but also because they display a completely different temporal development, indicating the occurrence of different processes. In the control runs, particulate activities first rise, then decrease slightly and rise again towards the end of the experiment. This evolution is not seen in any of the other experiments. We attribute the high particulate activities in the control run to the formation of particles in filtered natural seawater. This effect is known from other experiments using natural seawater (Chin et al., 1998). Compared to those experiments, particle formation here is enhanced by continuous stirring of the sample. The observed fraction of thorium on particles is sometimes even higher than typically reported for natural samples. Besides the formation of particles enhanced by stirring, the smaller pore size used here (0.2 μm) compared to most works on natural samples (1 μm) may also contribute to relatively high particulate activities in the control run, because smaller aggregates will be retained on the filter and attributed to the particulate phase.

The presence of clay (0.5 mg/L) led in all three runs to a relatively high particulate fraction of thorium (64–82% after more than 2 d). Highest Th activities on particles were observed for MnO_2 (around 90%). In some cases, lower activities were found on MnO_2 towards the end of the experiments. We conclude that loss of particles to the container walls was the reason because Protactinium activities are affected the same way in those samples, and recovery was low. The results for $CaCO_3$ differ strongly depending on the water type used. The particulate fraction on biogenic opal is for two cases surprisingly constant at ~30%, in one case constantly around 45% with the exception of the two last values, which we consider to be outliers. In contrast to the other particle types, an equilibrium seems to be established immediately, even faster than for MnO_2.

Comparing the findings from the different runs, our results

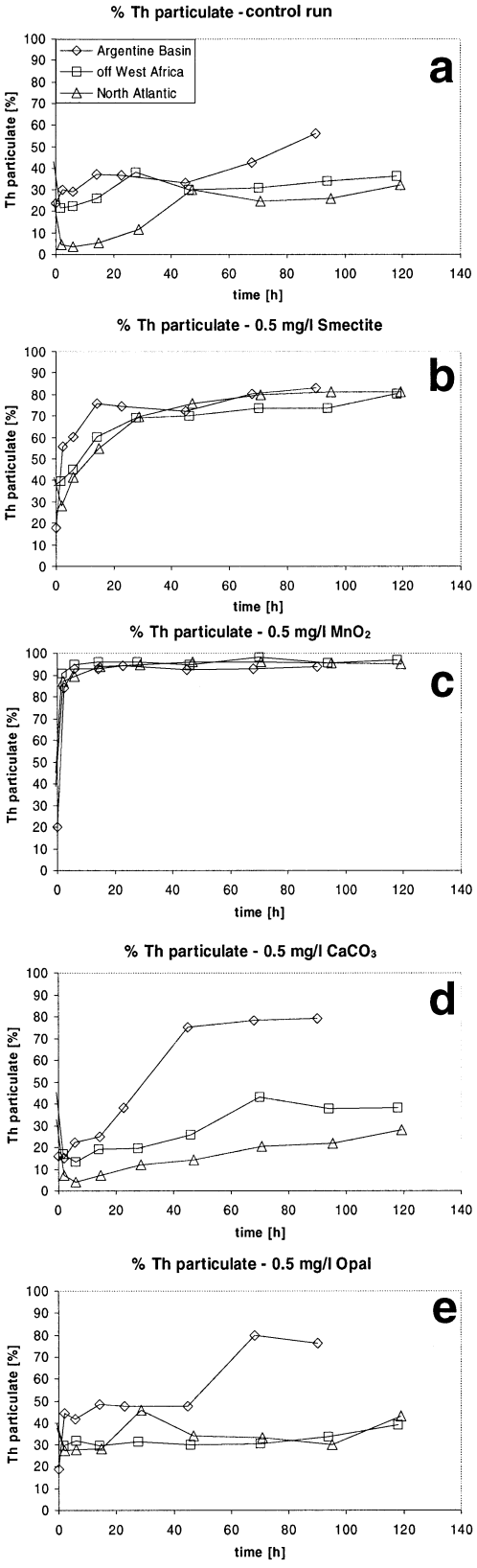

Fig. 2. The fraction of particulate thorium vs. time for five different particle types. Different symbols indicate water from different locations (see panel a for water type captions). Errors (1σ) are in general <3%.

suggest that the presence of some particle types in natural seawater may influence the process of particle formation by aggregation. A comparison of the control run to the carbonate and opal runs reveals that particle formation induced by stirring was reduced in some cases when $CaCO_3$ or biogenic opal were present. The few experiments presented here do not yet allow us to draw final conclusions, but they point towards an interesting aspect of particle formation. Currently, it remains speculative whether the effect is an experimental artefact or the reflection of a naturally occurring process.

The measured activities together with the known particle concentration allow the calculation of particle specific distribution coefficients (K_d-values) for the element:

$$K_d = \frac{\text{Activity}}{\text{g Particles}} \Big/ \frac{\text{Activity}}{\text{ml Solution}} \quad (1)$$

The concept of the K_d-value requires an equilibrium between dissolved and particulate phase. Obviously, in the beginning of the experiments the equilibrium is not yet established. The time needed for the equilibrium to be established depends on the particle types used. The decision whether equilibrium conditions were given had to be made for each sample individually, as indicated by bold types in Table 3. There, we give an overview of the obtained K_d-values for Thorium.

Highest K_d-values were found, just as expected, for MnO_2. These values have a quite large error due to the fact that dissolved activities are very low, thus adding a large measurement uncertainty to the final value. However, the mean K_d-value for Thorium on MnO_2 (as a precipitate with very fine grain-size) seems to be a robust estimate with 46×10^6 ml/g, considering the range of the results. It should be mentioned that this K_d-value may be an underestimate of the true value. Because virtually all Thorium available was adsorbed to particles, we cannot exclude that lower particle concentrations would also have led to a similar activity of Th on particles, and hence higher K_d-values.

The results for smectite are similar in all three runs. A mean K_d of 7.1×10^6 ml/g is obtained. The similarity of all three runs, the well established equilibrium and the still significant amounts of Th in the dissolved phase are supporting this value.

For biogenic opal, a mean K_d of 1.2×10^6 ml/g was calculated (excluding two outliers). Comparing the size of the *Thalassiosira* diatom frustrules used here to that of the clay or MnO_2 particles, one must conclude that the surface of biogenic opal is very reactive with respect to Thorium. This is supported by the very rapid establishment of the equilibrium. When the first subsample was taken after 2 h, the adsorption process was virtually completed.

For calcium carbonate, we give no overall mean K_d value because the three runs differ considerably. The results also differ considerably from the control runs, as seen in the graphs of Th_{part} vs. time (Fig. 2). However, the design of our experiment does not allow us to draw further conclusions on the reason for the different results. We did not observe changes in pH that correspond to the evolution of particulate Th in the carbonate run.

For the control run, we cannot give a K_d value because particle concentration is not known.

Table 3. The distribution coefficients (K_d in 10^6 ml/g) for Thorium on different particles vs. time elapsed since beginning of the experiments, in three different water types.[a]

Site	time (h)	Smectite	MnO_2	$CaCO_3$	Opal
Argentine Basin	2	2.64 ± 0.25	11.0 ± 1.1	0.36 ± 0.04	1.64 ± 0.15
	6	3.16 ± 0.29	27.6 ± 3.7	0.59 ± 0.06	**1.49 ± 0.14**
	14	**6.50 ± 0.58**	lost	0.69 ± 0.06	**1.96 ± 0.16**
	23	**6.13 ± 0.62**	**34.3 ± 6.0**	**1.29 ± 0.11**	**1.87 ± 0.18**
	45	**5.38 ± 0.46**	**26.0 ± 3.6**	**6.22 ± 0.59**	**1.88 ± 0.15**
	68	**8.45 ± 0.76**	**27.5 ± 3.6**	**7.46 ± 0.79**	8.13 ± 0.77[b]
	90	**10.19 ± 1.00**	**31.2 ± 4.6**	**7.92 ± 0.87**	6.60 ± 0.60[b]
	Mean K_d	**7.3**	**30**	**7.2**	**1.8**
	Range K_d[c]	**5.4–10.2**	**26–34**	**6.2–7.9**	**1.5–2.0**
Off West Africa	2	1.36 ± 0.11	19.8 ± 1.8	0.42 ± 0.04	0.87 ± 0.07
	6	1.70 ± 0.13	36.1 ± 4.2	0.32 ± 0.03	**0.96 ± 0.07**
	14	3.15 ± 0.24	50.3 ± 7.2	0.49 ± 0.04	**0.88 ± 0.07**
	28	**4.64 ± 0.40**	**49.1 ± 8.0**	0.51 ± 0.05	**0.95 ± 0.08**
	46	**4.82 ± 0.44**	**36.9 ± 5.4**	0.71 ± 0.05	**0.88 ± 0.07**
	70	**5.78 ± 0.49**	**106.7 ± 23.1**	**1.58 ± 0.13**	**0.90 ± 0.08**
	94	**5.82 ± 0.52**	**43.5 ± 6.7**	**1.25 ± 0.11**	**1.06 ± 0.09**
	118	**8.49 ± 0.84**	**69.5 ± 18.2**	**1.29 ± 0.11**	**1.32 ± 0.10**
	Mean K_d	**5.9**	**61**	**1.4**	**1.0**
	Range K_d[c]	**4.6–8.5**	**37–107**	**1.3–1.6**	**0.9–1.3**
North Atlantic	2	0.80 ± 0.07	13.8 ± 1.2	0.16 ± 0.02	0.77 ± 0.07
	6	1.47 ± 0.12	17.1 ± 2.2	0.09 ± 0.01	**0.80 ± 0.06**
	15	2.51 ± 0.21	30.7 ± 5.5	0.16 ± 0.02	**0.81 ± 0.07**
	29	4.73 ± 0.38	**38.0 ± 4.7**	0.28 ± 0.03	**1.74 ± 0.14**
	47	**6.49 ± 0.58**	**47.7 ± 9.0**	0.35 ± 0.03	**1.07 ± 0.08**
	71	**8.34 ± 0.79**	**48.0 ± 9.0**	**0.54 ± 0.04**	**1.03 ± 0.08**
	95	**9.05 ± 0.84**	**46.1 ± 8.3**	**0.58 ± 0.05**	**0.89 ± 0.07**
	119	**8.85 ± 0.82**	**39.8 ± 6.6**	**0.81 ± 0.07**	**1.57 ± 0.13**
	Mean K_d	**8.2**	**44**	**0.6**	**1.1**
	Range K_d[c]	**6.5–9.1**	**38–48**	**0.5–0.8**	**0.8–1.7**
	Mean K_d total	**7.1**	**46**	—	**1.2**
	Range K_d total[c]	**4.6–10.2**	**26–107**	**0.5–7.9**	**0.8–2.0**

[a] Errors are given as 1σ deviation, the calculation is including error propagation. For the control run, no K_d-value can be given because the particle concentration is unknown. For $CaCO_3$, no overall mean K_d value is given because the individual runs obviously belong to different populations. The values shown in bold type are assumed to represent equilibrium conditions. Only these values were included in the calculation of the mean K_d-values and the ranges. These numbers are given at the bottom for the individual water types, and in the bottom of the table for all water types.

[b] Excluded as an outlier.

[c] Rounded.

3.3. Protactinium on Different Particles

In general, protactinium is less particle reactive than thorium. The observed particulate fractions of Pa (Pa_{part}) range from 1 to 99%. Errors are larger than for thorium as a consequence of the measurement technique and the sometimes very low particulate activities. However, some clear results are obtained. In the control run, much less Pa than Th is found in the particulate phase. The results for Pa_{part} in the carbonate run are as low as in the control run.

Clear effects of adsorption were seen with MnO_2, smectite and biogenic opal. In the MnO_2 run, virtually all Pa was found in the particulate phase after more than 1 d. This result compares well to thorium. However, adsorption is evolving more slowly than for thorium, indicating that a particle concentration adsorbing less than all Pa might reveal a fractionation of Th and Pa by MnO_2.

In the smectite run (Fig. 3b), the fraction of Pa_{part} increases continuously until an equilibrium is reached after more than 3 d.

In contrast, the adsorption of Pa onto biogenic opal seems to take place immediately. Pa_{part} values on opal are lower than for smectite, though adsorption of Pa onto opal is faster than onto smectite.

The K_d-values for Pa as given in Table 4 are lower than those of Th, except on MnO_2. Also remarkable is the slower reaction of Pa with smectite and MnO_2, whereas a similar or faster reaction is found with calcium carbonate and biogenic opal.

3.4. Th/Pa Fractionation by Different Particles

The experimental determination of Th/Pa fractionation factors ($F_{Th/Pa}$) was one of the objectives of this work. The fractionation factor, describing the preferential uptake of an element or isotope compared to another, can be calculated as the ratio of their respective K_d-values.

Because the particle concentration cuts out in this calculation, our overview of $F_{Th/Pa}$ (Table 5) contains a column for the control run with unknown particle concentration, too. In the order of increasing fractionation, we obtain a value of 1.0 (no fractionation) for MnO_2, a value of 2.8 for opal, 5.4 for smectite, and 6.7 for the control run with particles presumably consisting of natural organic matter. For $CaCO_3$, we give no

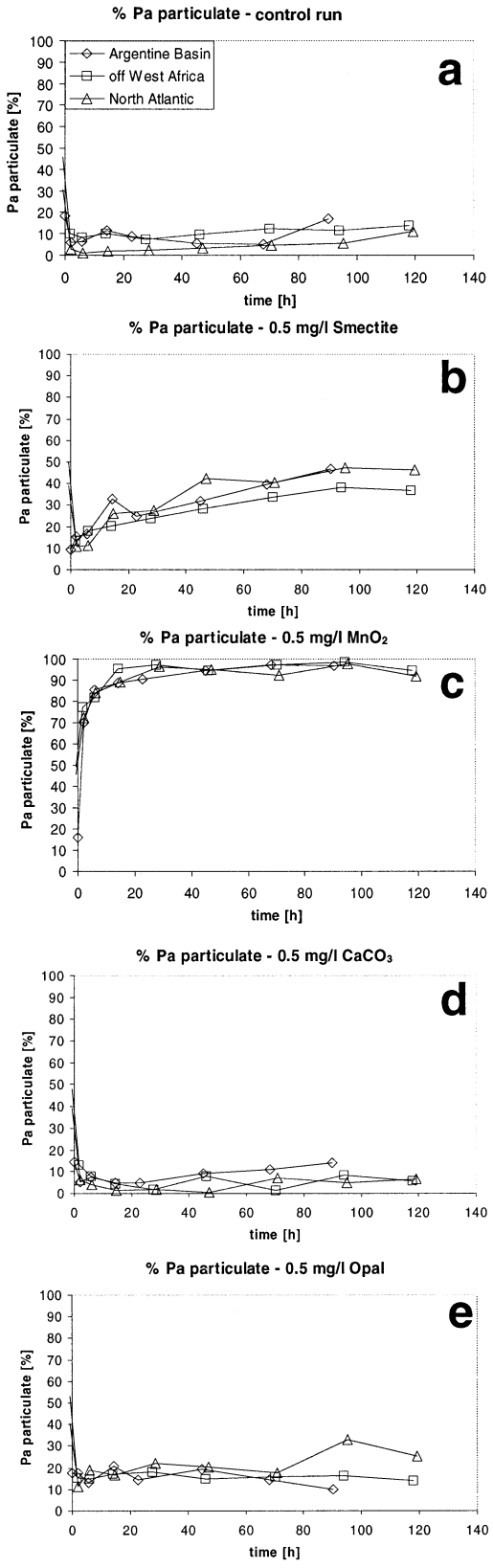

Fig. 3. The fraction of particulate protactinium vs. time for five different particle types. Different symbols indicate water from different locations (see panel a for captions). Errors (1σ) are in general <3%.

overall mean because the values are differing extremely, as indicated by the range.

4. DISCUSSION

4.1. Data Quality

Keeping in mind that no correction was made for additionally forming particles as observed in the control run, the F-factors have to be reconsidered carefully. For example, the value of 2.8 for opal is certainly an upper limit of its true F-Factor. Assuming that some additional particles with a much higher F-factor (6.7), as found in the control run, might have formed in this experiment too, the value for opal may be biased towards the F-factor of such particles. We therefore conclude that the F-factor of our biogenic opal is probably less than 2.8.

For MnO_2, the result ($F_{Th/Pa} = 1.0$) may be biased in the other direction. An influence of additional particles is unlikely, because the particulate fractions of Th and Pa were much higher than in the control run. Actually, virtually all Th and Pa was found on particles. Therefore a potential difference in the adsorption behaviour of Th and Pa might have been overlooked. Indeed, the somewhat slower adsorption of Pa onto MnO_2 points towards that possibility. Even lower concentrations of MnO_2 than our 0.5 mg/L would be required to resolve such a difference, if present.

For smectite, not much bias is to be expected because the F-factors of control run and smectite run are comparable. Furthermore, in the smectite run, a high fraction of the nuclides was found on particles, much more than in the control run but still enough to obtain reliable K_d values. Therefore, we expect the signal of smectite to dominate a potential signal of additionally present particles. Because all three runs with smectite have yielded very similar results, we have little doubt that 5.4 is a reasonable estimate of $F_{Th/Pa}$ for smectite in natural seawater from the sea surface.

The quality of the results for carbonate can not currently be assessed. Extreme variability between the runs make repeated experiments necessary to evaluate which effects are responsible for the variations.

We also give a value for $F_{Th/Pa}$ in the particles formed in the control run. In doing so, we implicitly assume that just one type of particle forms, and that an equilibrium would be established. This assumption probably does not hold true. However, the values obtained are not meaningless. Because all $F_{Th/Pa}$ values in the control run are far above unity, typically even higher than for smectite, we conclude that the organic particles which presumably form do fractionate thorium and protactinium strongly.

Another aspect of data quality here is the transferability of our values to the whole class of particles which they represent. We chose here just one (chemically treated) diatom to represent biogenic opal as a whole, smectite to represent the clay minerals, and a MnO_2 precipitate represent naturally formed brownstone. We certainly would expect different results for different diatoms, clay minerals, or forms of MnO_2. However, our results give an idea of the differing adsorption processes for different particle types. We expect results like the stronger Th/Pa fractionation on smectite compared to our biogenic opal to hold true in general for clay minerals compared to biogenic

Table 4. The distribution coefficients (K_d in 10^6 ml/g) for protactinium on different particles vs. time elapsed since beginning of the experiment.[a]

Site	time (h)	Smectite	MnO_2	$CaCO_3$	Opal
Argentine Basin	2	0.37 ± 0.04	4.8 ± 0.4	0.11 ± 0.02	**0.44 ± 0.04**
	6	0.41 ± 0.04	12.3 ± 1.1	0.17 ± 0.02	**0.31 ± 0.03**
	14	1.01 ± 0.09	lost	0.10 ± 0.01	**0.54 ± 0.05**
	23	0.68 ± 0.06	19.2 ± 1.9	0.11 ± 0.01	**0.35 ± 0.03**
	45	0.97 ± 0.08	**34.4 ± 3.2**	**0.21 ± 0.02**	**0.50 ± 0.04**
	68	1.35 ± 0.12	**76.3 ± 8.2**	**0.26 ± 0.03**	**0.35 ± 0.04**
	90	**1.84 ± 0.16**	**65.5 ± 6.9**	**0.34 ± 0.03**	**0.23 ± 0.02**
	Mean K_d	—	**59**	**0.27**	**0.39**
	Range K_d[b]	**(1.8)**	**34–76**	**0.21–0.34**	**0.2–0.5**
Off West Africa	2	0.33 ± 0.03	7.1 ± 0.6	0.32 ± 0.03	**0.38 ± 0.03**
	6	0.46 ± 0.04	9.2 ± 0.9	0.18 ± 0.02	**0.36 ± 0.03**
	14	0.53 ± 0.05	43.0 ± 4.4	0.09 ± 0.01	**0.43 ± 0.04**
	28	0.64 ± 0.06	**68.5 ± 7.8**	0.04 ± 0.01	**0.46 ± 0.05**
	46	0.83 ± 0.07	**37.5 ± 4.0**	**0.18 ± 0.02**	**0.37 ± 0.04**
	70	1.06 ± 0.10	**68.4 ± 8.2**	**0.03 ± 0.00**	**0.39 ± 0.04**
	94	**1.30 ± 0.12**	**165.9 ± 20.1**	**0.19 ± 0.02**	**0.40 ± 0.04**
	118	**1.22 ± 0.11**	**35.1 ± 3.9**	**0.13 ± 0.01**	**0.34 ± 0.03**
	Mean K_d	—	**75**	**0.13**	**0.39**
	Range K_d[b]	**1.2–1.3**	**35–166**	**0.03–0.19**	**0.3–0.5**
North Atlantic	2	0.25 ± 0.03	5.4 ± 0.5	0.14 ± 0.02	0.26 ± 0.03
	6	0.27 ± 0.03	10.8 ± 1.1	0.08 ± 0.01	**0.48 ± 0.05**
	15	0.73 ± 0.07	17.0 ± 1.8	0.03 ± 0.00	**0.41 ± 0.04**
	29	0.78 ± 0.08	**55.9 ± 7.0**	0.03 ± 0.01	**0.59 ± 0.06**
	47	1.51 ± 0.15	**41.1 ± 5.5**	0.01 ± 0.00	**0.53 ± 0.05**
	71	1.41 ± 0.13	**25.0 ± 2.8**	**0.15 ± 0.02**	**0.44 ± 0.04**
	95	**1.86 ± 0.17**	**96.2 ± 12.4**	**0.11 ± 0.01**	**1.01 ± 0.09**
	119	**1.78 ± 0.16**	**23.9 ± 3.0**	**0.14 ± 0.02**	**0.70 ± 0.07**
	Mean K_d	—	**48**	**0.13**	**0.59**
	Range K_d[b]	**1.8–1.9**	**24–96**	**0.11–0.15**	**0.4–1.0**
	Mean K_d total	**1.6**	**61**	**0.17**	**0.5**
	Range K_d total[b]	**1.2–1.9**	**24–166**	**0.03–0.34**	**0.4–1.0**

[a] Errors are given as 1σ deviation, the calculation is including error propagation. For the control run, no K_d-value can be given because the particle concentration is unknown. The values shown in bold type are assumed to represent equilibrium values. Only these values were included in the calculation of the mean K_d-values and the ranges. When only one or two values were available (smectite), no mean could be calculated.
[b] Rounded.

opal. This expectation is based not only on our own results, but also on other results obtained by different approaches.

4.2. Comparison with Other Results

Only a few values for Th/Pa distribution are available in the literature that may be directly compared with our results. The best comparison is possible with the recent work of Chase et al. (2002). There, pseudo-K_d-values (K_d*) for Th and Pa (and Be, which is not considered here) in natural sediment trap material are calculated, derived from the production of the nuclides in the overlying water column. These values compare well to our experimental findings, although they are based on a completely different calculation approach.

The K_dTh and K_dPa values of Chase et al. (2002) are in the same range as ours. Chase et al. (2002) give a value of 4.8×10^6 (g/g) for Th, and 5.7×10^5 (g/g) for Pa as an overall mean for the natural particle mixtures. This compares well to our results in Table 3 and Table 4, disregarding MnO_2. Looking at the data in more detail regarding the K_ds of individual particle types, Chase et al. (2002) give values for biogenic opal and carbonate that may be compared to ours. Chase et al. report a value for K_dTh on opal of 0.39×10^6 (this work: 1.2×10^6), and a K_dPa on opal of 1.4×10^6 (this work: 0.5×10^6). For carbonate, they give a K_dTh of 9.0×10^6 (this work: $0.5–7.9 \times 10^6$), and K_dPa of 0.22×10^6 (this work: 0.17×10^6). The approach of Chase et al. derives K_d from the relation of Pa and Th found on particles in sediment traps to the Pa and Th inventory in the overlying 1000 m water column. To obtain K_d values for individual particle types, they use stations which reasonably represent a two end-member mixing situation, and extrapolate K_d for one end-member. Obviously, this approach also gives rise to uncertainties, e.g., the 1000-m assumption, the variability in the empirical relationships, or the extrapolation to single end-members. However, considering the uncertainties in their approach as well as in our own, the results agree reasonably well, and both studies show some similar trends. The results of Chase et al. (2002) suggest that $F_{Th/Pa}$ of a pure biogenic opal end-member would approach unity. Our results are not inconsistent with this idea, considering the conclusions about data quality for the opal run. For carbonate, the high variability in our data does not allow a detailed comparison. Concerning the importance of clay minerals for the scavenging process, our results seem to show a discrepancy to Chase et al. (2002) at first. Whereas our experiments point to a strong adsorption of Th onto clay, the data set of Chase et al. seems to show virtually no correlation between %lithogenic and K_dTh. However, looking more closely at their background data set,

Table 5. Overview of $F_{Th/Pa}$ vs. time for the different particle types and water types.[a]

Site	Time (h)	Control run	Smectite	MnO_2	$CaCO_3$	Opal
Argentine Basin	2	6.67 ± 1.02	7.14 ± 1.02	2.28 ± 0.30	3.28 ± 0.60	3.70 ± 0.50
	6	6.20 ± 0.96	7.65 ± 1.02	2.26 ± 0.36	3.40 ± 0.54	**4.80 ± 0.67**
	14	4.65 ± 0.62	6.40 ± 0.83	lost	6.79 ± 1.02	**3.66 ± 0.45**
	23	5.95 ± 0.82	9.04 ± 1.22	1.79 ± 0.36	11.86 ± 1.69	**5.27 ± 0.71**
	45	**8.39 ± 1.10**	5.55 ± 0.66	**0.76 ± 0.13**	**29.69 ± 3.93**	**3.79 ± 0.46**
	68	**14.49 ± 2.23**	6.26 ± 0.79	**0.36 ± 0.06**	**28.72 ± 4.24**	23.35 ± 3.24[b]
	90	**6.20 ± 0.86**	**5.55 ± 0.73**	**0.48 ± 0.09**	**23.59 ± 3.46**	29.25 ± 3.92[b]
	Mean F	**9.7**	**(5.6)**	**0.5**	**27.3**	**4.4**
	Range F[c]	**6–14**	**(5.6)**	**0.4–0.8**	**24–30**	**3.7–5.3**
Off West Africa	2	2.47 ± 0.31	4.16 ± 0.50	2.80 ± 0.34	1.32 ± 0.16	2.30 ± 0.28
	6	3.14 ± 0.40	3.68 ± 0.44	3.93 ± 0.60	1.82 ± 0.24	**2.69 ± 0.33**
	14	3.10 ± 0.39	5.99 ± 0.70	1.17 ± 0.20	5.31 ± 0.71	**2.04 ± 0.24**
	28	7.76 ± 1.07	7.22 ± 0.90	**0.72 ± 0.14**	12.30 ± 1.94	**2.08 ± 0.27**
	46	**4.05 ± 0.53**	5.84 ± 0.74	**0.98 ± 0.18**	4.05 ± 0.54	**2.41 ± 0.30**
	70	**3.11 ± 0.43**	5.46 ± 0.68	**1.56 ± 0.39**	**53.62 ± 7.71**	**2.33 ± 0.30**
	94	**3.99 ± 0.56**	**4.49 ± 0.58**	**0.26 ± 0.05**	**6.67 ± 0.95**	**2.66 ± 0.36**
	118	**3.60 ± 0.48**	**6.99 ± 0.93**	**1.98 ± 0.56**	**10.10 ± 1.37**	**3.87 ± 0.49**
	Mean F	**3.7**	**5.7**	**1.1**	—	**2.6**
	Range F[c]	**3–4**	**4.5–7.0**	**0.3–2.0**	**7–54**	**2.0–3.9**
North Atlantic	2	1.72 ± 0.35	3.17 ± 0.42	2.54 ± 0.32	1.17 ± 0.20	**2.99 ± 0.40**
	6	4.62 ± 1.01	5.55 ± 0.71	1.59 ± 0.26	1.07 ± 0.19	**1.66 ± 0.21**
	15	3.40 ± 0.56	3.43 ± 0.43	1.80 ± 0.38	5.81 ± 0.99	**1.97 ± 0.25**
	29	6.08 ± 1.12	6.05 ± 0.78	**0.68 ± 0.12**	8.32 ± 1.55	**2.94 ± 0.39**
	47	**13.06 ± 1.87**	4.29 ± 0.58	**1.16 ± 0.27**	44.92 ± 7.33	**2.02 ± 0.25**
	71	**6.75 ± 0.92**	5.90 ± 0.78	**1.92 ± 0.42**	**3.46 ± 0.47**	**2.35 ± 0.29**
	95	**6.18 ± 0.92**	**4.87 ± 0.63**	**0.48 ± 0.11**	**5.39 ± 0.80**	**0.88 ± 0.11**
	119	**3.90 ± 0.54**	**4.98 ± 0.65**	**1.66 ± 0.35**	**5.57 ± 0.79**	**2.24 ± 0.29**
	Mean F	**7.5**	**4.9**	**1.2**	**4.8**	**2.0**
	Range F[c]	**4–13**	**4.9–5.0**	**0.5–1.9**	**3–6**	**0.9–2.9**
	Mean F total	**6.7**	**5.4**	**1.0**	—	**2.8**
	Range F total[c]	**3–14**	**4.5–7.0**	**0.3–2.0**	**3–54**	**0.9–5.3**

[a] For the calculation of F, equilibrium values for both isotopes are required. This condition was assumed to be sufficiently met in the cases shown in bold type. Only these values were included in the calculation of the mean values. The best estimate for general applications is the overall mean value given at the bottom of the table.
[b] Excluded as an outlier.
[c] Rounded.

especially at the samples with a low content of lithogenic matter, a strong correlation between K_dTh and %lithogenic is found in their data as well. This correlation is only found in open ocean environments with their low particle concentrations, and this is the water type that we used for our experiments. From their results, it also seems likely that the difference between open ocean and ocean margin plays a major role for the partitioning of Th and Pa between the particulate and dissolved phases. Open ocean values and ocean margin values obviously belong to different populations. This idea is consistent with our finding of different relationships in different water types.

An experimental setup comparable to ours, although with different particle types, may be found in Nyffeler et al. (1984). They studied the adsorption of Th and Pa (besides other radiotracers) onto fecal pellets and sediment trap material over a longer period (up to 110 d). They obtain for $F_{Th/Pa}$ a value of ~10 (sediment trap material), and ~5 (fecal pellets, calculated from fig. 3 in Nyffeler et al., 1984). The lack of characterization of the material used by Nyffeler et al. prevents a closer comparison with the particle types used in this work, although the values for $F_{Th/Pa}$ are comparable to the clay and the control run in this work.

Another experimental approach to the adsorption behaviour of Pa and Th on different particles is reported by Guo et al. (2002). This work also presents evidence for large differences between different particle types. So far, most results are quantitatively comparable to our own approach, especially the results for MnO_2, and -in part- carbonate. Contrasting results are obtained for SiO_2, where we found much higher adsorption of thorium than they did, still exceeding that of Pa. However, the experiments of Guo et al. differ largely from our setup in several aspects. In particular, three main differences make a direct comparison with our experiments difficult. First, particle concentrations of Guo et al. (2002) were a factor of 200 higher, presumably leading to very small dissolved fractions of the added nuclides. Second, equilibrium conditions in Guo et al. were assumed to be met after 2 h, whereas we consider here a time span of several days. Third, Guo et al. performed the experiments in artificial seawater, which will probably have little effect when using high particle concentrations as they did, but may be a major difference at low particle concentrations as observed in natural marine systems. Some of their results point to interesting aspects of Th/Pa scavenging behaviour that were not examined here, such as strong adsorption on acid polysaccharides. Further experiments will be needed to see in how far the two approaches can be compared.

Earlier publications had already pointed to a particular role of biogenic opal for enhanced Pa scavenging (Lao et al., 1992; Walter et al., 1997). These findings, based on empirical rela-

tionships observed in natural systems, are supported by our own results, although they are less pronounced than expected.

Two recent publications report an inverse relationship between $^{231}Pa/^{230}Th$ ratios and ^{232}Th activities (Luo and Ku, 1999; Narita et al., 2003). In both works, this relationship is explained by a preferential uptake of ^{230}Th by lithogenic particles, assuming ^{232}Th concentration to be a direct measure of the lithogenic fraction of particles. Although we also find a strong adsorption of Th onto clay, other results of these studies are only partially supported here. For example, the conclusion that biogenic phases do serve to a minor extent as scavengers for Th, and that high $^{231}Pa/^{230}Th$ ratios are determined by the relative absence of clay can not be confirmed from our results. We found substantial fractions of Pa on clay, and rapid Th adsorption is observed when biogenic opal is present. However, a comparison is difficult because strongly differing definitions were applied in the two studies.

Hirose (1995) and Hirose and Tanoue (1994a,b) found evidence for vertical variations within the water column in the Thorium complexing capacity of marine particulate matter. These findings point to possible variations in Th-adsorption depending on the type of seawater used. Our results support the idea of differing behaviour of Thorium in seawater from different locations, although we did not vary depth in our experiments, but only the geographical provenance of seawater.

4.3. The Potential Influence of the Provenance of Seawater

When planning the experiments, a potential influence of the type of seawater used was expected. This expectation was based on earlier observations on the large fraction of Th on colloids (Baskaran et al., 1992; Guo et al., 1997), the strong chemical bond of thorium onto some fractions of particles or colloids (Hirose, 1995; Quigley et al., 2001, 2002), and the known interaction between colloidal and particulate fractions. Indeed, a fraction of Th typically classified as dissolved must be expected to be adsorbed onto colloids (Tsunogai et al., 1994). Therefore, an adsorption of "dissolved" thorium onto particles in our experiments may also reflect the adsorption of colloids onto particles.

A first indicator for the connection of Th to the colloidal phase is the small fraction of Th adsorbed onto the container walls as evidenced by our good recoveries. These findings support the results of Baskaran et al. (1992), who found that the presence of colloids reduces losses to the container walls.

Because surface waters are known to be variable in their colloidal composition (e.g., Benner, 2002), an effect of different water types was to be expected. Pronounced differences between water types were found in the carbonate runs, the opal runs, and the control runs. We conclude that the K_d-values and the fractionation factor of thorium and protactinium should not only be considered to be a function of particle type, but also of the seawater used.

In deeper waters, less influence of the water types would be expected because the dissolved organic carbon (DOC) content of deep waters is less variable than in surface waters. However, a potential influence of the composition of seawater itself may be expected for ocean margins compared to open ocean systems, and shallow waters compared to deep waters, or in regions with recently downwelled surface water coming into contact with sediments (like e.g., the Weddell Sea Bottom Water [WSBW]).

4.4. Implications for Paleoenvironmental Applications

Our results do not allow the identification of one distinct particle type acting as a main carrier phase for thorium. An exception would be MnO_2, if present. All investigated particle types showed a considerable affinity for thorium. Smectite as a representative of clay would adsorb a large fraction of thorium. Considering the large surface of clay particles, this effect is not surprising. Opal also adsorbed a considerable fraction of thorium. Remarkable here was the very quick response of the equilibrium to the presence of opal. The new equilibrium was established much faster than for smectite. For carbonate, all kinds of responses were found, ranging from low to very high particulate activities. Some very high particulate activities here also point to a potential role of carbonate as a carrier phase for Th. To a certain extent, we consider the control run to give information on organic carbon, because the particles observed were most likely of organic composition. If these results reflect the behaviour of organic carbon with respect to thorium, this phase must be considered to be a very strong scavenger. Neglecting MnO_2, the observed K_d-values for thorium were all within one order of magnitude. The K_d of Th on clay differs from the K_d on opal by a factor of 6.

The normalization of sediment accumulation rates to thorium fluxes or the normalization of individual sediment components by means of thorium rely to a certain extent on the homogeneous distribution of thorium between different particle types. This correction by normalizing often provides a possibility to correct for the strong effects of sediment redistribution. Our findings suggest that no phase is the exclusive carrier of thorium in the sediment. Comparing the possible bias introduced by inhomogenous distribution of thorium in the sediment to the improvement of information from the marine sedimentary record obtained by Th normalization, we conclude that Th normalization is an excellent tool to give improved estimates of true oceanic fluxes.

Concerning the known constraints on the use of the sedimentary $^{231}Pa/^{230}Th$ ratio as a proxy for particle fluxes, the results presented here do not offer a solution. The question to which extent varying Pa/Th ratios in the sediment may be due to particle composition can only be addressed tentatively from our results. Indeed, $F_{Th/Pa}$ was found to be lower for opal than for clay, just as proposed earlier (Lao et al., 1992; Walter et al., 1997), and recently shown by Chase et al. (2002). However, compared to the expected $F_{Th/Pa}$ of unity on opal, and of about 10 on clay (Walter et al., 1999; Chase et al., 2002), the difference between clay and opal found here is only a factor of two ($F_{Th/Pa} = 2.8$ for opal vs. 5.4 for smectite). Considering the constraints of the experimental approach (opal leached by acid and hydrogen peroxide; use of surface water; smectite as a representative for clay), our results may be seen as confirming the trend indicated by measurements on natural particles (Chase et al., 2002).

A variable that has been newly introduced here is the provenance and composition of seawater. Some results suggest that Th/Pa fractionation may not only be a function of the particle

type, but also of the water in which the adsorption occurs. It remains to be tested in the future whether this observation holds for deeper waters, too.

5. CONCLUSIONS

The experimental approach with natural, recently sampled seawater offers a new key to the understanding of the adsorption of thorium and protactinium onto natural particles. This approach provides the advantage of good recoveries even for a strongly particle reactive element like thorium. This type of experiment more closely mimics natural conditions by including colloids which are known to play a crucial role in thorium cycling.

The difficulties encountered (mainly the formation of particles in the control runs) may not only be seen as difficulties, but also as a challenge for future investigations. The process of particle formation from the dissolved phase certainly occurs naturally (see Chin et al., 1998), although to a lesser extent, and has to be taken into account when investigating particle cycling at the sea surface.

All particle types investigated displayed their own characteristic adsorption kinetics, pointing to different mechanisms of adsorption. Whereas adsorption onto biogenic opal took place immediately and changed very little later on, adsorption onto clay was slower, but finally larger. Similarities in the temporal evolution of Th adsorption onto clay and in the control run may point to a common underlying mechanism in both cases. Further experiments especially designed to solve this question are needed to confirm and explain this similarity.

Now addressing the first of our three questions from the beginning of this work, our results suggest that in the sediment, no individual phase investigated here would serve as a main carrier of thorium (except MnO_2, if present), but that more thorium will be found in the smaller grain sizes. However, we observed here that opal also adsorbed considerable amounts of thorium in spite of its much larger grain size compared to clay. This is an encouraging finding concerning the use of ^{230}Th as a constant flux proxy.

Concerning the influence of particle composition on the ^{231}Pa/^{230}Th ratio, our results confirm the trend of earlier observations that opal fractionates Pa and Th less than clay. They also suggest that an influence of particle composition would have to be expected in the sediment.

The differences found between the three runs with different water types must be ascribed to variations in the composition of the dissolved phase, because the other conditions were kept constant. This implies that when thorium is used to investigate particle cycling near the sea surface, attention should be paid to the dissolved phase. In surface waters, variations in the dissolved phase may be controlling the adsorption of thorium onto particles, together with variations in particle composition.

Acknowledgments—Thanks to Michiel M. Rutgers van der Loeff and Hans-Jürgen Dauelsberg who inspired this work from the very beginning, and to Roger François for kindly sharing his knowledge on the subject. Thanks also to Dieter K. Fütterer for supporting the project. The crew of RV *Polarstern* was very helpful during the experiments. Jörg Hofmann, Claudia Hanfland, Ingrid Vöge, Jens Riefstahl, and Jill Schwarz also contributed to this work. Augusto Mangini, Zanna Chase and an anonymous reviewer provided useful comments to an earlier version of this work.

Associate editor: S. Krishnaswami

REFERENCES

Anderson R. F., Bacon M. P., and Brewer P. G. (1983a) Removal of ^{230}Th and ^{231}Pa from the open ocean. *Earth Planet. Sci. Lett.* **62,** 7–23.

Anderson R. F., Bacon M. P., and Brewer P. G. (1983b) Removal of ^{230}Th and ^{231}Pa at ocean margins. *Earth Planet. Sci. Lett.* **66,** 73–90.

Baskaran M., Santschi P. H., Benoit G., and Honeyman B. D. (1992) Scavenging of thorium isotopes by colloids in seawater of the Gulf of Mexico. *Geochim. Cosmochim. Acta* **56,** 3375–3388.

Benner R. (2002) Chemical composition and reactivity. In *Biogeochemistry of Marine Dissolved Organic Matter* (eds. D. A. Hansell and C. A. Carlson), pp. 59–90. Academic Press.

Buesseler K. O., Bacon M. P., Cochran J. K., and Livingston H. D. (1992) Carbon and nitrogen export during the JGOFS North Atlantic Bloom Experiment estimated from ^{234}Th: ^{238}U disequilibria. *Deep-Sea Res.* **39,** 1115–1137.

Burd A. B., Moran S. B., and Jackson G. A. (2000) A coupled adsorption-aggregation model of the POC/^{234}Th ratio of marine particles. *Deep-Sea Res. I* **47,** 103–120.

Chase Z., Anderson R. F., Fleisher M. Q., and Kubik P. W. (2002) The influence of particle composition and particle flux on scavenging of Th, Pa and Be in the ocean. *Earth Planet. Sci. Lett.* **204,** 215–229.

Chase Z., Anderson R. F., Fleisher M. Q., and Kubik P. W. (2003a) Scavenging of ^{230}Th, ^{231}Pa and ^{10}Be in the Southern Ocean (SW Pacific Sector): The importance of particle flux, particle composition and advection. *Deep-Sea Res. II* **50,** 739–768.

Chase Z., Anderson R. F., Fleisher M. Q., and Kubik P. W. (2003b) Accumulation of biogenic and lithogenic material in the Pacific sector of the Southern Ocean during the past 40,000 years. *Deep-Sea Res. II* **50,** 799–832.

Chin W.-C., Orellana M. V., and Verduco P. (1998) Spontaneous assembly of marine dissolved organic matter into polymer gels. *Nature* **391,** 568–572.

Coale K. H. and Bruland K. W. (1985) ^{234}Th-^{238}U disequilibria within the California Current. *Limnol. Oceanogr.* **30,** 22–33.

Cochran J. K. and Masqué P. (2003) Short-lived U/Th series radionuclides in the ocean: Tracers for scavenging rates, export fluxes and particle dynamics. In *Reviews in Mineralogy and Geochemistry* 52 (eds. B. Boudron, et al.). pp. 461–492. Uranium-Series Geochemistry.

François R., Bacon M. P., Altabet M. A., and Labeyrie L. D. (1993) Glacial/interglacial changes in sediment rain rate in the SW Indian sector of subantarctic waters as recorded by ^{230}Th, ^{231}Pa, U, and δ^{15}N. *Paleoceanography* **8,** 611–629.

Frank M., Gersonde R., and Mangini A. (1999) Sediment redistribution, $^{230}Th_{ex}$-normalization and implications for the reconstruction of particle flux and export paleoproductivity. In *Use of Proxies in Paleoceanography: Examples from the South Atlantic* (eds. G. Fischer and G. Wefer), pp. 409–426. Springer.

Guo L., Santschi P. H., and Baskaran M. (1997) Interaction of thorium isotopes with colloidal organic matter in oceanic environments. *Colloids Surf. A* **120,** 255–271.

Guo L., Hung C. C., Santschi P. H., and Walsh I. D. (2002) ^{234}Th scavenging and its relationship to acid polysaccharide abundance in the Gulf of Mexico. *Mar. Chem.* **78,** 103–119.

Guo L., Chen M., and Gueguen C. (2002) Control of Pa/Th ratio by particulate chemical composition in the ocean. *Geophys. Res. Lett.* **29,** 1961.

Henderson G. and Anderson R. F. (2003) The U-series toolbox for paleoceanography. In *Reviews in Mineralogy and Geochemistry* 52 (eds. B. Boudron, et al.). pp. 493–531. Uranium-Series Geochemistry.

Hirose K. and Tanoue E. (1994a) Thorium-particulate matter interaction: Thorium complexing capacity of oceanic particulate matter—Theory. *Geochim. Cosmochim. Acta* **58,** 1–7.

Hirose K. and Tanoue E. (1994b) The vertical distribution of the strong ligand in particulate organic matter in the North Pacific. *Mar. Chem.* **59,** 235–252.

Hirose K. (1995) The relationship between particulate uranium and thorium-complexing capacity of oceanic particulate matter. *Sci. Total Environ.* **173/174,** 195–201.

Honeyman B. D., Balistrieri L. S., and Murray J. W. (1988) Oceanic trace metal scavenging: The importance of particle concentration. *Deep-Sea Res.* **35,** 227–246.

Honeyman B. D. and Santschi P. H. (1989) A Brownian-pumping model for oceanic trace metal scavenging: Evidence from Th isotopes. *J. Mar. Res.* **47,** 951–992.

Kumar N., Gwiazda R., Anderson R. F., and Froelich P. N. (1993) $^{231}Pa/^{230}Th$ ratios in sediments as a proxy for past changes in Southern Ocean productivity. *Nature* **362,** 45–48.

Kumar N., Anderson R. F., Mortlock R. A., Froelich P. N., Kubik P., Dittrich-Hannen B., and Suter M. (1995) Increased biological productivity and export production in the glacial Southern Ocean. *Nature* **378,** 675–680.

Lao Y., Anderson R. F., Broecker W. S., Trumbore S. E., Hofmann H. J., and Wolfli W. (1992) Transport and burial rates of ^{10}Be and ^{231}Pa in the Pacific ocean during the Holocene period. *Earth Planet. Sci. Lett.* **113,** 173–189.

Li Y.-H., Burkhart L., Buchholtz M., O'Hara P., and Santschi P. H. (1984) Partition of radiotracers between suspended particles and seawater. *Geochim. Cosmochim. Acta* **48,** 2011–2019.

Luo S. and Ku T.-L. (1999) Oceanic $^{231}Pa/^{230}Th$ ratio influenced by particle composition and remineralization. *Earth Planet. Sci. Lett.* **167,** 183–195.

Marchal O., François R., Stocker T. F., and Joos F. (2000) Ocean thermohaline circulation and sedimentary $^{231}Pa/^{230}Th$ ratio. *Paleoceanography* **15,** 625–641.

Morel A. (1996) An ocean flux study in eutrophic, mesotrophic and oligotrophic situations: The EUMELI program. *Deep-Sea Res. I* **43,** 1185–1190.

Narita H., Abe R., Tate K., Kim Y., Harada K., and Tsunogai S. (2003) Anomalous large scavenging of ^{230}Th and ^{231}Pa controlled by particle composition in the northwestern North Pacific. *J. Oceanogr* **59,** 739–750.

Nour S., Burnett W. C., and Horwitz E. P. (2002) ^{234}. Th analysis in marine sediments via extraction chromatography and liquid scintillation counting. *Appl. Radiation Isotopes* **57,** 235–241.

Nyffeler U. P., Li Y. H., and Santschi P. H. (1984) A kinetic approach to describe trace-element distribution between particles and solution in natural aquatic systems. *Geochim. Cosmochim. Acta* **48,** 1513–1522.

Quigley M. S., Santschi P. H., Guo L., and Honeyman B. D. (2001) Sorption irreversibility and coagulation behavior of ^{234}Th with marine organic matter. *Mar. Chem.* **76,** 27–45.

Quigley M. S., Santschi P. H., Hung C.-C., Guo L., and Honeyman B. (2002) Importance of acid polysaccharides for ^{234}Th complexation to marine organic matter. *Limnol. Oceanogr.* **47,** 367–377.

Rutgers van der Loeff M. M., Friedrich J., and Bathmann U. (1997) Carbon export during the spring bloom at the southern Polar Front, determined with the natural tracer ^{234}Th. *Deep-Sea Res. II* **44,** 457–478.

Rutgers van der Loeff M. M., Meyer R., Rudels B., and Rachor E. (2002) Resuspension and particle transport in the benthic nepheloid layer in and near Fram Strait in relation to faunal abundances and ^{234}Th depletion. *Deep-Sea Res. I* **49,** 1941–1958.

Suman D. O. and Bacon M. P. (1989) Variations in Holocene sedimentation in the North American Basin determined from ^{230}Th measurements. *Deep-Sea Res.* **36,** 869–878.

Thomson J., Colley S., Anderson R., Cook G. T., MacKenzie A. B., and Harkness D. D. (1993) Holocene sediment fluxes in the Northeast Atlantic from $^{230}Th_{excess}$ and radiocarbon measurements. *Paleoceanography* **8,** 631–650.

Tsunogai S., Nozaki Y., and Minagawa M. (1974) Behavior of heavy metals and particulate matters in seawater expected from that of radioactive nuclides. *J. Oceanogr. Soc. Jpn.* **30,** 251–259.

Tsunogai S. and Minagawa M. (1976) Vertical flux of organic materials estimated from Th-234 in the ocean (abstract). In *Book of Abstracts, Joint Oceanographic Assembly, Edinburgh,* p. 156. FAO.

Tsunogai S., Kawasaki M., and Harada K. (1994) Different partitioning among Thorium isotopes in seawater of the Northern North Pacific. *J. Oceanogr.* **50,** 197–207.

Usman K. and MacMahon T. D. (2000) Determination of the half-life of ^{233}Pa. *App. Radiation Isotopes* **52,** 585–589.

Walter H.-J., Rutgers van der Loeff M. M., and Hoeltzen H. (1997) Enhanced scavenging of ^{231}Pa relative to ^{230}Th in the South Atlantic south of the Polar Front: Implications for the use of the $^{231}Pa/^{230}Th$ ratio as a paleoproductivity proxy. *Earth Planet. Sci. Lett.* **149,** 85–100.

Walter H. J., Rutgers van der Loeff M. M., and François R. (1999) Reliability of the $^{231}Pa/^{230}Th$ activity ratio as a tracer for bioproductivity of the ocean. In *Use of Proxies in Paleoceanography: Examples from the South Atlantic* (eds. G. Fischer and G. Wefer), pp. 393–408. Springer.

Wen L. S., Santschi P. H., and Tang D. (1997) Interactions between radioactively labeled colloids and natural particles: Evidence for colloidal pumping. *Geochim. Cosmochim. Acta* **61,** 2867–2878.

Yu E.-F., François R., and Bacon M. P. (1996) Similar rates of modern and last-glacial ocean thermohaline circulation inferred from radiochemical data. *Nature* **379,** 689–694.